

# Simulation of Laserwire in BDS

G. Penn\*, CERN, Geneva, Switzerland

## Abstract

The laser wire scanner (LWS) is a non-destructive beam diagnostic which has been proposed for CLIC and other very low emittance electron beams. Measurements of the beam size can be made with resolutions below a micron. Two configurations for detecting scattered electrons are simulated, and the signals compared with the backgrounds resulting from expected halo losses. The requirements of the LWS are compared with conditions in the CLIC beam delivery system.

## 1 INTRODUCTION

The laser wire scanner (LWS) has been proposed as a diagnostic in CLIC and other very low emittance electron beams. Diagnostics to measure the beam are needed to commission the lattice, to optimize performance, and for physics experiments. The LWS is rapid, non-destructive (small total cross section), and can be used to measure the relative number of electrons intersecting the laser beam. If the laser width is sufficiently small, this allows for a transverse density scan, but does not directly measure beam angles. LWS promises submicron resolution and, unlike true wires, all of the hardware is well separated from the beam and so protected from damage. There are, however, concerns about how to detect the scattered electrons or photons, and about background levels. Because of the collimation and much larger beta functions in parts of the beam delivery system (BDS), the requirements for the LWS are examined in terms of BDS parameters to determine what, if any, constraints a laser wire scanner would impose on the BDS.

## 2 COMPTON SCATTERING

The Compton scattering process can be analyzed most simply by examining the physics in the rest frame of the electrons. We consider a laser with frequency  $\nu$  intersecting an electron beam with energy  $E_B = m_e c^2 \gamma_B$ . In the electron rest frame, the photon is upshifted by  $\gamma_B$  (or  $2\gamma_B$  if originally antiparallel), to the frequency  $\nu' \simeq \gamma_B \nu$ . The scattering process in the electron frame depends on the Compton parameter [1]  $\xi = h\nu'/m_e c^2$ . In the Thomson regime,  $\xi \ll 1$ , the photon energy is still less than the electron rest mass, and the collision will be nearly elastic. Photons which are backscattered then get upshifted by another factor of  $2\gamma_B$  in the lab frame. Thus, scattered photons have frequencies as high as  $2\gamma_B^2 \nu$  with angles  $< 1/\gamma_B$ . The electrons, however, are only slightly affected by the interaction. In the Compton regime,  $\xi \gtrsim 1$ ,

the photon can acquire most of the electron's energy, although the final electron energy is at least  $m_e^2 c^4 / 2h\nu$ , so that the final  $\gamma > \gamma_B / 2\xi$ . The typical angle for scattered photons, which is also the maximum angle of electrons, is  $\sim \xi / \gamma_B \simeq h\nu / m_e c^2$ . Electrons at the largest scattering angle have energy  $\sim \gamma_B m_e c^2 / \xi$ .

The main demands for LWS are to have a large signal and good resolution. The spread of the laser beam can be subtracted from the measured size of the beam, but the effectiveness of this is limited by how well the laser is characterized, and the shape of the electron beam modifies the correction as well. The total number of scattering events depends on the electron beam only through its spatial distribution and energy. The dimensions of the electron beam are given as  $\sigma_x, \sigma_y$ , and  $\sigma_z$ , while the laser pulse will be defined by its wavelength  $\lambda = c/\nu$ , duration  $\tau_L$ , peak power  $P_L$ , and minimum spot size  $\sigma_{L0}$ . The spot size  $\sigma_{L0}$  is the rms in intensity of the laser at its focus, which is half of the "waist" in laser terminology. Considering a measurement of the profile in  $y$ , the conditions for accurate measurement of the electron beam are  $\lambda < \sigma_{L0} < \sigma_y$ , and  $\sigma_y / \sigma_x > M^2 \lambda / 2\pi \sigma_{L0} = \text{angle of laser cone}$ . The quantity  $M^2$  is the ratio of the Rayleigh length of an ideal, single-mode Gaussian beam to the actual Rayleigh length due to the presence of higher order modes. If the laser satisfies

$$c\tau_L \gg \sigma_{L0}, \sigma_x, \quad (1)$$

the number of scattering events scales as

$$N_{\text{scat}} \propto N_e P_L \frac{\lambda}{\sigma_y} \frac{c\tau_L}{(c^2\tau_L^2 + \sigma_z^2)^{1/2}} \frac{\lambda}{E_B}, \quad (2)$$

where  $N_e$  is the total number of electrons in the bunch. The last factor only applies in the Compton scattering regime. To maximize the signal, it is preferable to take as large  $\lambda$  and  $\tau_L$  as is consistent with the desired resolution. To detect degraded electrons, it is also necessary to be in the Compton regime with large  $\xi = h\nu'/m_e c^2 \simeq 5E_B [\text{TeV}] / \lambda [\mu\text{m}]$ . Then for higher energies, more laser power will be needed to obtain the same signal.

## 3 LASER WIRE SCANNER SIMULATIONS

The scattering of electrons by the laser beam is easily simulated, and the resulting particles have been tracked in several simplified detector and magnetic field geometries. In addition, more sophisticated GEANT simulations have been used to model interactions with materials and the detection process itself. The following have been taken as preliminary parameters for the CLIC beam at the intersection with the laser: 0.67 nC charge per bunch,  $E_B = 1.5$

\*gregory.penn@cern.ch

TeV,  $\sigma_x = \sigma_y = 20\mu\text{m}$ , and  $20 \times 680\text{ nm}$  normalized emittance. Typical angles are 0.3 nrad vertical and 11 nrad horizontal, and are completely negligible together with the small energy spread of order 160 MeV. Thus, for such small emittances, the signal from the LWS is sensitive only to the physical size of the beam.

For the laser, we have taken  $0.25\mu\text{m}$  wavelength,  $5\mu\text{m}$  width, with energy of 1 mJ per pulse. The pulse duration of 0.12 ps matches the  $35\mu\text{m}$  bunch length of the electron beam. The scattering parameters are  $h\nu/m_e c^2 \simeq 10^{-5}$ , and  $\xi \simeq 30$ . Under these conditions there are roughly 3000 scattering events per pulse. For the diagnostics, a 1 m long gas detector was placed next to the beam pipe; upon impact of the degraded electrons with the beam pipe, secondaries are produced which deposit energy into the detector. Two magnetic configurations were considered: a pair of strong sextupoles at 20 and 40 m; and a continuous, 100 gauss dipole field.

For a beam energy of 1.5 TeV, the distribution of scattered electrons and photons are shown in Figures 1 – 3. There is a large population of electrons with energy in the range 50 – 150 GeV, with their corresponding photons which acquire the bulk of the original electron energy. This also corresponds to a peak in scattered angle of the electrons at  $10\mu\text{radians}$ . The photon distribution, on the other hand, peaks at angles of less than  $1\mu\text{radian}$ . The two magnetic configurations loosely correspond to selection based on scattering angle for the sextupoles, and based on energy for the dipole field.

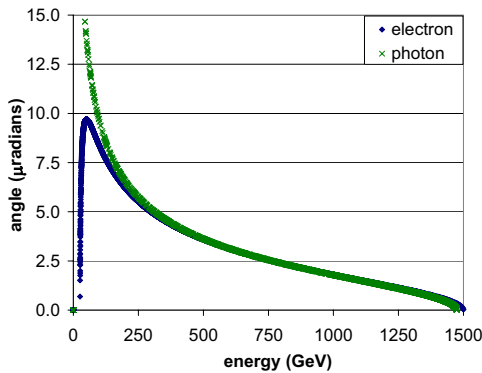


Figure 1: Distribution of scattered electrons and photons.

In Figures 4 and 5, the extraction of the degraded electrons is examined in terms of the rate at which particles hit the beam pipe for the sextupole and dipole magnetic fields, respectively. Results are given in terms of number of electrons (right hand scale) and total energy deposited (left hand scale). Note that in the dipole field case, the beam pipe is still assumed straight, so that the large deposition of high energy particles at large  $z$  actually marks the point at which the beam pipe should be shifted transversely by one radius. In the proper configuration, this would be where the signal from the photons might be observed. In the more realistic GEANT simulations shown below, the beam pipe

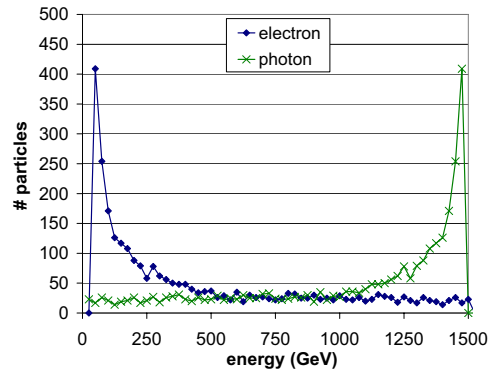


Figure 2: Histogram of scattered electrons and photons by energy, in 25 GeV bins.

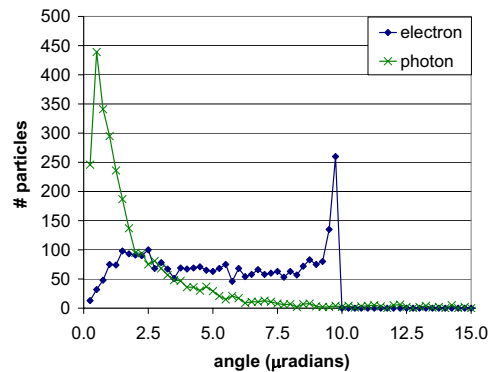


Figure 3: Histogram of scattered electrons and photons by angle, in  $1/4\mu\text{radian}$  bins.

is curved appropriately for the dipole field.

From these results, we see that degraded electrons can be swept out of the beam by magnetic fields with a reasonable efficiency. Using short sextupoles, there is a sharp peak in losses against the beam pipe which contains 15% of scattered electrons, but is less peaked in terms of energy. On the other hand, using a long dipole field, there are more particles contained within the peak, but the resulting signal will be similar to secondaries produced by lost halo particles because of the shallow angles produced by the uniformly weak magnetic field.

The extraction of particles by the sextupole magnets is not as effective as using a simple dipole field. In part, this is because the sextupole field acts oppositely in different azimuthal regions, leading to particles being swept to different sides of the beam pipe depending on their initial direction after scattering. In addition, by examining the scattering angles weighted by particle energy instead of by number as in Figure 3, we see in Figure 6 that the peak in the distribution for large angle scatters is not nearly so pronounced in terms of energy. Considering as well the care with which sextupoles must be placed in such a low emittance beam, this suggests that sextupoles are not a practical method for extracting the LWS signal. By comparison, the

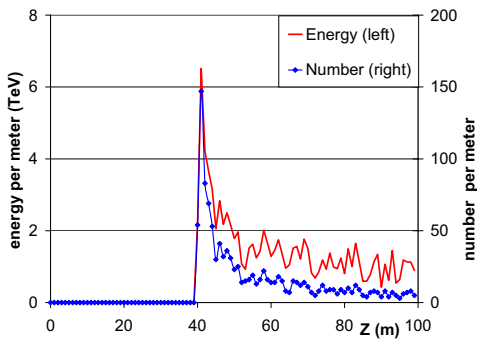


Figure 4: Location in  $z$  of intersection of degraded electrons with beam pipe, with sextupoles located at  $z = 20$  m and 40 m.

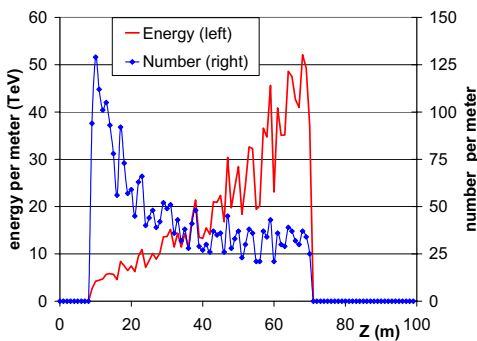


Figure 5: Location in  $z$  of intersection of degraded electrons with beam pipe, with uniform dipole field of 100 gauss.

dipole fields are a simple design which works well, and fields of 100 gauss are not very disruptive even for TeV range electron beams. Lower magnetic fields can be used, but the rate of particles detected per meter drops significantly.

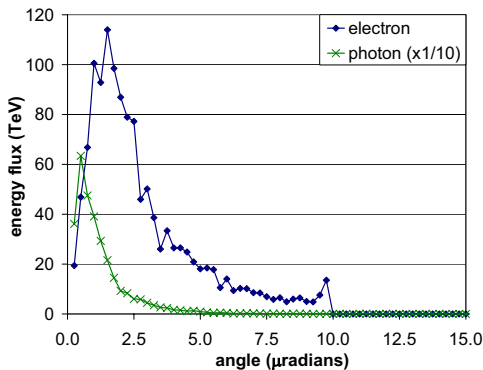


Figure 6: Histogram of scattered electrons and photons by angle, weighted by electron energy, in  $1/4$   $\mu$ radian bins.

## 4 ESTIMATE OF BACKGROUNDS

To analyze the usefulness of these schemes, it is necessary to also consider the backgrounds introduced by beam losses, which occur throughout the beam line. The backgrounds are estimated to be the result of a loss of a single halo electron hitting the beam pipe every meter. This very low loss rate probably limits the LWS to be used after some sort of beam collimation. The BDS, one of whose essential functions is beam collimation, is thus a reasonable place to attempt to situate the laser wire system. In addition to these schemes, it may also be possible to detect the scattered, up-shifted photons. There, the signal must be separated from halo losses and from synchrotron radiation, although here shielding can be quite effective.

Simulations in GEANT allow for issues of detection and backgrounds to be addressed in a realistic way. The results are here presented in Table 1 in terms of energy deposited in the detector, for the degraded electrons and as well for the halo particles, assuming a nominal loss rate of 1 per meter. This corresponds to a time average of 3.7 mW per meter for the CLIC bunch structure. The results for a calculation of beam losses performed by G. Blair (Ref. [2]), given a  $10^{-3}$  beam halo fraction, is illustrated in Figure 7. Several regions are apparent which fall below the 4 mW level of power deposition. An iron shielding block placed in front of the detector is seen to improve the ratio of signal to background. Without the shielding in front of the detector, halo losses from far upstream can lead to hits in the detector. A similar shield placed behind the detector, however, provided no benefit.

The background is caused by the spray of secondaries from halo losses. For sextupoles, where there are large bending angles, it may be possible to further improve the sensitivity to the signal based on particle direction. The best case considered so far is a 1 m long shielded gas detector in a dipole field, yielding a signal to noise ratio of 7. Approximately 100 degraded electrons produced significant hits, defined by excluding those electrons which deposited less than half of the average value into the detector. This corresponds to an efficiency of 4%, which is low but still reasonable. The consequences of such low statistics will be examined more closely below. Because the detector response time will probably be longer than the time between electron bunches, the signal from the LWS will have to compete against halo losses from multiple bunches in the train; assuming a detector response time of 3 ns, this implies an enhancement in background by a factor of 4 but no corresponding enhancement in the signal. This effect will reduce the achievable signal to noise ratio by a factor of 4 from the results given above, to below 2.

The above results were for a detector placed 15 m after the laser wire, and with the laser wire aligned to maximize the signal. The laser power was taken to be 1 mJ per pulse. For a 250 nm wavelength, this is already a challenging power requirement. The design parameters are compared against commercially available lasers in Table 2. The “ef-

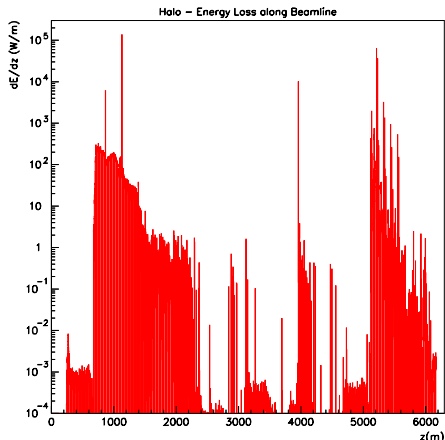


Figure 7: Simulated beam halo losses in the CLIC beam delivery system, in terms of power deposited per meter. From G. Blair, Ref. [2].

Table 1: Signal and background calculations in GEANT.

Magnets and Detector	Signal	Background
sextupoles, shielded Pb	65	120
sextupoles, shielded gas	0.14	0.10
dipole, unshielded gas	0.78	0.20
dipole, shielded gas	0.35	0.05
500 GeV, dipole	1.8	0.065

fective energy” is defined to be the equivalent energy of a laser overlapping a single bunch, as in the design parameters, necessary to yield the same rate of scattering events. Thus, the effectiveness of the Nd:YAG laser is enhanced by the fact that it overlaps multiple bunches, but reduced by the low repetition rate. The Ti:Sapphire laser must go through a frequency tripler before intersecting the beam, which reduces the available power by an order of magnitude. We see that achieving the design parameters will require either custom-built lasers or will rely on future advancements in available laser technology. For short laser pulses, proper synchronization between the laser and the electron bunch may also be an issue. However, the results for the Ti:Sapphire laser may be overly pessimistic because the available pulse length and interval between pulses are both much shorter than is necessary; relaxing these conditions may allow for significantly greater energy per pulse. Yet even the design parameters yielded only moderate signal to background ratios and low statistics, so clearly further work is required on optimising both the detector and the shielding.

For comparison, laser wire scanner experiments from CTFII operated in the Thomson regime by using a 2.5 mJ laser at 1 micron wavelength to measure a 50 MeV electron beam [3]. In this case, the upshifted laser light is de-

Table 2: Laser parameters compared with commercial lasers.

	Design	Nd:YAG	Ti:Sapphire
wavelength	250 nm	266 nm	800 nm
pulse FWHM	150 fs	3 ns	50 fs
energy per pulse	1 mJ	200 mJ	0.7 mJ
rep rate	100 Hz	10 Hz	1 kHz
energy fluct	-	8%	1%
peak power	5 GW	0.05 GW	1 GW
effective energy	1 mJ	0.015 mJ	0.1 mJ

tected; for the experimental geometry used, about 600 photons were expected to hit the detector with each laser pulse. At the lowest noise levels experienced in the beam, the ratio of expected signal to the measured backgrounds was approximately 1:8. Even with these low statistics and large level of noise, by averaging over several scans the backgrounds could be subtracted out sufficiently to observe the profile of the electron beam. Although consistent with the known beam profile, the resolution was still too low for an accurate measurement. Below, we will examine more quantitatively the achievable accuracy of the profile measurement for different signal and background levels.

## 5 RECONSTRUCTION OF BEAM SIZE AND EMITTANCE

Because of the finite spot size of the laser, the LWS will not directly yield the true profile of the beam, but will depend on the laser properties as well. Diffraction of the laser beam will also affect the measured beam size. Under the assumptions of Eq. (1), together with the condition that

$$\sigma_R \equiv \frac{\lambda M^2 \sigma_x}{2\pi \sigma_{L0}} \ll \sigma_y, \quad (3)$$

we can approximate the contributions to the measured beam radius as

$$\sigma_{\text{meas}}^2 \simeq \sigma_y^2 + \sigma_{L0}^2 + \sigma_R^2. \quad (4)$$

The quantity  $\sigma_R$  represents the additional effective size of the laser beam due to its diffraction, if the Rayleigh range of the laser is comparable to the horizontal size of the beam. Fluctuations due to background and to low statistics will further complicate the calculation of the beam size. The first correction can easily be kept below 10%, and the laser waist can be measured accurately. The second term, due to diffraction of the laser beam, is more difficult to determine with a high accuracy, and should be kept below a few percent. These conditions essentially determine the maximum wavelength light which can be used for a high accuracy measurement, and are equivalent to the conditions given in Section 2.

It is possible to observe these constraints in the CLIC BDS, and so we assume that systematic effects such as the

Table 3: Reconstructions of beam size.

Ratio, background to peak signal	Fluctuations in:			$\sigma_y$ due to background
	peak signal	fitted peak	$\sigma_y$	
0	2.2%	0.9%	2%	-
0.1	2.5%	1%	2.6%	1.7%
0.25	3.0%	1.6%	4.1%	3.6%

contribution from  $\sigma_{L0}$ , etc., can be accurately subtracted out. The process of reconstructing  $\sigma_y$  is then examined under the following assumptions: the peak signal, when the laser is centered, consists of 2000 detected particles; the fluctuations in the signal are purely statistical; and background fluctuations of 10%, which is larger than the purely statistical level. The laser wire scan consists of 10 measurements taken across the beam; thus, a single scan of the beam profile would take 0.1 s. The “measured” beam size was then calculated using a basic parametric fit to a Gaussian, allowing for displacements and a constant background. The results are shown in Table 3.

More generally, we find the following:

- In the absence of backgrounds, the error in  $\sigma_y$  is roughly the inverse square root of the peak number of particles detected. The statistical fluctuations in the tails are worse than this, but there may in fact be a better algorithm for reconstructing  $\sigma_y$ .
- Backgrounds introduce additional errors, on the order of  $1.5 \times (\text{background fluctuations}) / (\text{peak signal})$ . This error adds in quadrature to the statistical error from the signal itself.
- The reconstructed peak line density has half the statistical error of the width  $\sigma_y$  when there are no backgrounds. With backgrounds, this difference is even more pronounced.
- The emittance is equal to  $\sigma_y^2 / \beta_y$ ; the fluctuations in measuring  $\sigma_y^2$  can be kept below 5% for a signal to noise ratio  $\geq 10$ . In fact, at this level the statistical noise in the signal itself is the most significant problem.

Because of this last point, any method which acquires more statistics can improve performance, even if the backgrounds are enhanced as well, so long as the signal to noise ratio of 10:1 can be achieved. Thus, although current simulations using the design parameters have yielded around 100 hits in the detector per scan, this can be scaled up to 2000 hits by doubling the length of the detector and by measuring 100 bunches per scan instead of 10. The penalty for this is that each emittance measurement would take 1 second.

Because the beam may not be exactly matched, a full emittance diagnostic would need to consist of a combination of measurements at different beam phases, which would then be combined into an emittance measurement.

Because the LWS is non-destructive, these measurements can be performed simultaneously. In general,  $\sigma_y^2$  must be measured at three locations, but for small mismatch it is expected that the combined error will be less than twice that of the individual measurements. This implies that, so long as three suitable locations can be found, an accuracy of 10% in the beam emittance should be possible, although both the laser power and the LWS design need improvements, and each scan may require 1 second to complete.

## 6 CONCLUSIONS

More simulations and optimization must be done to properly assess the requirements of a laser wire scanner for the CLIC beam. The possibility of detecting photons should also be explored further. Conditions in the BDS seem favourable for the inclusion of this diagnostic, although it is unclear whether a pair of such locations separated by  $\pi/2$  will be readily available. At least two locations are necessary for measuring the emittance, and a third location is desirable to be able to account for a large beam mismatch. The size of the beam in the BDS is sufficient for the measurements; in fact, the total LWS cross-section becomes larger for smaller electron beams.

Because smaller electron beams produce a larger signal, it may be desirable to locate the LWS at a position where the beam is significantly smaller, perhaps  $5 - 8 \mu\text{m}$ . The signal can also be enhanced by using longer wavelengths for the laser, as is apparent from Eq. (2), although this will increase the minimum energy of the degraded electrons, and thus the detector geometry will have to be adjusted. Lowering the laser frequency has the added benefit of avoiding power losses due to the inefficiency of upshifting laser light which is produced in the  $800 \text{ nm} - 1 \mu\text{m}$  range. For full flexibility, to be able to measure the beam over a range of emittances and conditions, the LWS should probably be designed to operate at both 250 nm and 500 nm wavelengths. Even at  $1 \mu\text{m}$  wavelength, the required resolution may be achievable for beams which are at least several microns wide. As seen in Table 3, another option to improve statistical errors is to measure the peak line density rather than the beam size. Rather than yielding emittance, this would depend on the phase space density in the core of the beam, which may be as useful for optimizing luminosity.

Future work will focus on improving the geometry of the LWS detection system, as well as adjusting the beam and laser parameters, in order to achieve the desired signal and resolution. The backgrounds may need to be reduced by further collimation or more extensive shielding of the detector. A more sophisticated detector which would be capable of reconstructing tracks and determining particle energies may be able to distinguish between hits due to halo losses and hits due to degraded electrons. The required laser power is a concern, but the requirements should decrease with further optimization. Because a major difficulty is with poor statistics, more measurements per emit-

tance scan can resolve this difficulty at the expense of a longer measurement time. For the current configuration, for a detector with a time resolution of 3 ns, the overlap of halo losses from adjacent bunches will result in a signal to noise ratio which is far too low, at approximately 2:1. Thus, the LWS may paradoxically require smaller beam sizes in order to obtain the desired 10% accuracy in emittance. A single measurement of beam emittance in one plane may require scanning up to 100 pulses, over a period of 1 second.

## 7 REFERENCES

- [1] T. Lefevre, "Laser Wire Scanner: Basic Process and Perspectives for the CTFS and CLIC Machines", CLIC Note CERN-OPEN-2002-010, and references therein.
- [2] G. Blair, "Simulation of Laserwire in BDS", in these proceedings.
- [3] J. Bossert, H.H. Braun, E. Bravin et al., "Laser Wire Scanner Development on CTFIP", paper TU411 in *Proceedings of the Linac 2002 Conference*, Gyeongju, Korea, 2002.